ELSEVIER

Journal of Molecular Structure 559 (2001) 67–77

Journal of
MOLECULAR
STRUCTURE

www.elsevier.nl/locate/molstruc

Molecular orbital calculations, experimental and theoretical UV spectra of granulatimides and didemnimides, biologically active polycyclic heteroaromatic alkaloids from the ascidian *Didemnum granulatum*

A.J. Camargo, J.H.H.L. Oliveira, M. Trsic*, R.G.S. Berlinck

Instituto de Química de São Carlos, Universidade de São Paulo, CP 780, 13560-970, São Carlos, SP, Brazil

Received 2 March 2000; accepted 12 June 2000

Abstract

A detailed computational study was performed for compounds granulatimide, isogranulatimide, and didemnimides A, D, and E, using the semiempirical Austin model 1 quantum chemical method. The electronic features and structural parameters were confronted with the inhibition of the G2 cell cycle checkpoint of mammalian cancer cells. All compounds were submitted to a rigorous conformational analysis using the Tripos 5.2 force field implemented in the Spartan 5.01 program. The electronic density in specific regions of the molecules appears to play a pivotal role towards activity. The molecular planarity creates a broad negative electrostatic potential on the two sides of the active compounds (granulatimide and isogralulatimide) and a positive potential in their central core, while the non-planar compounds (didemnimides A, D, and E, which are inactive) present an asymmetric potential scattered over the molecules. These electrostatic potential features are likely to be the modulator of hydrophobicity or lipophilicity of the compounds, which appear correlated with activity. The hydrogen attached to the N atom of the pyrrole moiety of indole is more positive for active compounds than for the inactive molecules. The theoretical electronic spectra were obtained for all compounds using the configuration interaction method, with the AM1 routine. All transitions present $\pi \rightarrow \pi^*$ nature. The theoretical results are in good agreement with experimental values.

Keywords: Granulatimides; Didemnimides; Electronic spectra; Quantum chemistry; Marine invertebrates

1. Introduction

Ascidians (Phylum Chrodata, Sub-Phylum Urochordata) are marine invertebrates with a chemically rich secondary metabolism. Amino acid derivatives, such as alkaloids and peptide derivatives, are the main group of ascidian natural products which very often display potent biological activities [1–6].

Recently, some of us reported the identification and synthesis of the novel polycyclic alkaloids isogranulatimide (1) and granulatimide (2), isolated from the ascidian *Didemnum granulatum*, collected in the Brazilian coastline [7] (see in Fig. 1 the respective chemical structures). Both isogranulatimide and granulatimide selectively inhibited the G2 cell cycle checkpoint of mammalian cancer cells, but normal

* Corresponding author. Tel./fax: +55-16-273-9975.
E-mail addresses: milan@iqsc.sc.usp.br (M. Trsic), rberlinck@iqsc.sc.usp.br (R.G.S. Berlinck).

0022-2860/01/$ - see front matter
PII: S0022-2860(00)00681-5

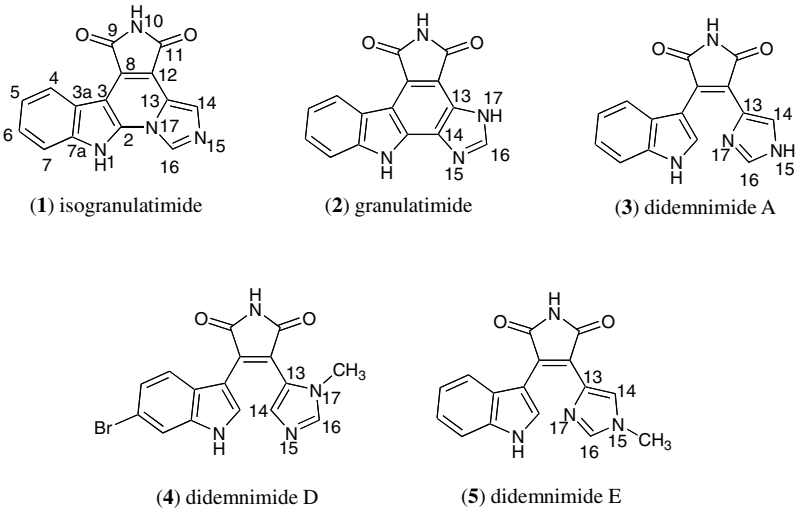

Fig. 1. The chemical structures for the *D. granulatum* alkaloids under study.

cells were affected to a much smaller extent [8]. Therefore, the granulatimide alkaloids are considered as a novel class of potentially useful compounds for cancer treatment.

Besides the isolation of isogranulatimide and granulatimide, the structurally related didemnimides A (3), D (4), and E (5) have also been isolated from *D. granulatum* (Fig. 1). The didemnimides A, B, C and D have been previously isolated from another ascidian species, *Didemnum conchyliatum* [9]. The didemnimides A, D and E proved to be inactive as cell cycle checkpoint inhibitors.

In order to initiate a quantitative structure–activity relationship (QSAR) study on the granulatimide and didemnimide alkaloids as cell cycle checkpoint inhibitors, we have performed molecular orbital calculations for isogranulatimide (1), granulatimide (2), and didemnimides A (3), D (4), and E (5).

Herein we report the results obtained with various theoretical approaches, as described in Sections 3 and 4. We also report the experimental electronic spectra of the species under study, as described in Sections 2 and 4.

2. Experimental

Isogranulatimide and didemnimides A, D and E have been isolated from the ascidian *D. granulatum*, as previously described [7]. Granulatimide was obtained by synthesis, as described earlier [7]. The ultraviolet spectra of isogranulatimide, granulatimide, didemnimide A, D, and E have been obtained using a HITACHI U3501 equipment. Solutions in millimolar concentrations were prepared in spectroscopic grade methanol (Aldrich), and the spectra were recorded at 25°C.

3. Computational procedure

The structures of the didemnimides A, D, and E, shown in Fig. 1, are very flexible. They present rotation around the bonds between the atoms C_3–C_8 and C_{12}–C_{13} which allows the possible existence of several conformations. To establish the most stable conformation as the initial point for further calculations, the molecules were submitted to a rigorous conformational analysis around the free rotation bonds. This study was performed with the software SPARTAN 5.01 [10] running on an Origin 2000 Workstation. The method used was the Tripos 5.2 force field [11].

The size of the molecules imposes several restrictions on the level of the quantum-mechanical method used for the description of the electronic and geometric properties. In practical terms, our option is limited to a semiempirical approach. The

semi-empiric hamiltonian AM1 [12] was the general procedure employed in the present work. This routine is implemented in the computational package AMPAC6.0 [13] running on ULTRASPARC SUN SOLARIS. The geometry for all compounds was fully optimized using the keyword PRECISE, which increases the precision of the calculation. When the norm of the gradient did not converge to a value below of the standard limit, the optimization process was restarted with the additional keyword NLLSQ, which is a non-linear method. Thus, it is expected that the obtained geometries are the best theoretically possible.

The atomic charges presented in this work were derived from the electrostatic potential. The model is based in the calculation of a set of punctual atomic charges defined around the molecule [14,15].

The electrostatic potential is a molecular property accessible directly from SCF calculations. The value of the potential calculated by quantum theory at point $\vec{r}_p$ for a system formed of N electrons and M nuclei is defined as being the electrostatic force that acts on an unitary positive charge in this point,

$$V^{q} = \sum_{a}^{M} \frac{Z_a}{|\vec{r}_p - \vec{R}_a|} - \sum_{\mu,\nu}^{N} P_{\mu\nu} \int \frac{\varphi_\mu \varphi_\nu}{|\vec{r}_p - \vec{r}|} d\vec{r} \quad (1)$$

where Z_a represents the nuclear charge of atom a centered in $\vec{R}_a$, V^{q} represents the potential calculated by quantum theory at point $\vec{r}_p$, the quantities $P_{\mu\nu}$ are the electron-density matrix elements or the charge-density, and φ_μ and φ_ν are the basis functions used. The first term in Eq. (1) corresponds to the contribution of the total potential due to the nuclei, where Coulomb's law is used to calculate the repulsion potential between the positive punctual charges Z_a and the unitary charge at the point $\vec{r}_p$. The second term is due to the potential of electrostatic attraction involving the distribution of electronic charges in the overall space and the unitary positive charge $\vec{r}_p$.

The electrostatic potential calculated quantum-mechanically, can also be approached using a set of punctual atomic charges (q_a) according to Coulomb's law,

$$V^{c} = \sum_{a} \frac{q_a}{r_{ap}} \quad (2)$$

where V^{c}represents the potential calculated using Coloumb's law, r_{ap} is the distance between the a-th nucleus and point $\vec{r}_p$, where the quantum electrostatic potential is being calculated. The atomic charges in Eq. (2) are defined in such a way that V^{c} reproduces V^{q} calculated according the Eq. (1). The least-squares method can be used to minimize the sum

$$\Delta = \sum_{p=1}^{L} (V_p^{q} - V_p^{c})^2 \quad (3)$$

where L is the number of points around the molecule used in the calculation. Therefore, it is necessary to choose a set of points around the molecule for the calculation of the electrostatic potential and posterior adjustment to the model of punctual charges. Points whose distances to the nuclei are smaller than the van der Waals radius are refused, because the proximity with the nuclei causes enormous distortions. Various methodologies have been proposed for the choice of the point distribution [16,17]. In the present work we used the routine developed by Connolly [18], which takes in account a density of 1 point per $Å^2$ in four distinct layers placed at distances of 1.4, l.6, 1.8, and 2.0 times the van der Waals radius. The charges derived from the energy potential have the advantage that they are physically more satisfactory than Mulliken's charges [19]. This procedure for charge calculation is of special relevance in simulations of intermolecular interactions [20], especially to describe molecules with biological activity.

The calculations for the electronic transitions were carried out through the configuration interaction (CI) method with the AM1 routine. For all molecules, the number of active orbitals for the CI were 20, i.e., they involved the region from HOMO − 9 to LUMO + 9. Single excitations were used for the CI calculation. Theoretical spectra were simulated considering the values of wavelength and oscillator strength for each transition.

Molecular Electrostatic Potential (MEP) maps for all molecules were calculated using SPARTAN's graphic module for the AM1-optimized geometries. The MEP isoenergy contours were generated in the range from −50.0 to −10.0 kcal/mol. The electrostatic potentials were sampled over the entire accessible surface of a molecule (corresponding roughly to a van der Waals contact surface) and in the space extending beyond the molecular surface providing a

Table 1
Frontier molecular orbital energies, partition coefficient, dipole moment and steric properties

	Didemnimide A	Didemnimide D	Didemnimide E	Isogranulatimide	Granulatimide
C_2–C_3–C_8–C_{12}[a]	34.83	−25.25	41.34	0.03	0.28
C_3–C_8–C_{12}–C_{13}	7.06	−6.42	3.35	−0.03	−0.56
C_8–C_{12}–C_{13}–N_{17}	13.21	−37.61	−8.87	−0.02	
Volume (Å^3)	292.28	336.75	314.43	280.84	279.79
Area (Å^2)	291.90	334.27	317.43	282.84	281.29
μ (debye)	2.39	3.53	5.75	4.99	6.26
HOMO−2 (eV)	−9.28	−9.41	−9.05	−9.76	−9.94
HOMO−1 (eV)	−9.17	−9.28	−8.79	−9.40	−8.99
HOMO (eV)	−8.32	−8.46	−8.01	−8.35	−8.81
LUMO (eV)	−1.48	−1.54	−1.02	−1.57	−1.16
LUMO + 1 (eV)	−0.02	−0.30	0.37	−0.83	−0.88
LUMO + 2 (eV)	0.46	0.23	0.66	0.09	0.22
log *P* (Dixon)	1.48	2.77	1.95	1.10	1.10
$\Delta\epsilon$ (eV)	6.84	6.92	6.99	6.78	7.65
ΔH_f (kcal/mol)	72.81	86.02	79.68	90.28	68.14

[a] The dihedral angles were measured in degrees.

measure of charge distribution from the point of view of an approaching reagent. The regions of positive electrostatic potential indicate excess positive charge, i.e., repulsion for the positively charged test probe, while regions of negative potential indicate areas of excess negative charge, i.e., attraction of the positively charged test probe. Three-dimensional isosurfaces of the MEPs at the van der Waals contact surface represent potentials superimposed onto a surface of constant electron density (0.002*e*/au^3).

4. Results and discussion

4.1. Geometry and molecular orbital analysis

The geometries of the molecules under study were optimized as described in Section 3. As a result, the didemnimide A (3), didemnimide D (4) and didemnimide E (5) molecules (Fig. 1) belong to the C_1 point group. Isogranulatimide (1) and granulatimide (2) (Fig. 1) are almost planar. The hydrogen bonded to the nitrogen N_1 atom is 0.1 Å out of plane for granulatimide and 0.8 Å for isogranulatimide, when fully optimized in vacuum. If those minimal geometry distortions were disregarded then the granulatimide and isogranulatimide should belong to the C_S point group.

All the molecular orbitals (MOs) analyzed (from HOMO − 9 to LUMO + 2), present π symmetry and are delocalized over the molecules; exceptionally, HOMO − 5 of the didemnimide E is a n_π orbital. The orbitals extending from HOMO − 9 to HOMO are bonding. The LUMO orbital is antibonding for all the compounds studied. The electron density distribution for HOMO and LUMO is basically the same for all the compounds considered. The presence of a methyl group in didemnimides D and E does not modify the electronic density distribution of the frontier orbitals in relation to the others compounds. Table 1 shows the energies for HOMO, LUMO, and $\Delta\epsilon$ ($\epsilon_{LUMO} - \epsilon_{HOMO}$) values for all the compounds. There is a difference of 0.8 eV between the highest (didemnimide E) and lowest (granulatimide) energy of the HOMO and there is a difference of 0.14 eV between the highest (didemnimide E) and lowest (granulatimide) energy of the LUMO. The methyl groups in didemnimides D and E do not promote a significant variation on the frontier orbital eigenvalues either. The most pronounced effect appears when the methyl group is bonded to the nitrogen atom. However, the methyl group produces significant modification in the molecular geometries, when compared with didemnimide A. Analysis of Table 1 illustrates this point. The compounds granulatimide and isogranulatimide are almost planar, a structural feature that appears to be a necessary condition for the expression of biological activity as G2 cell cycle

Table 2
Calculated and measured lowest electronic transitions for the *D. granulatum* alkaloids

Compound	Nature of the tranisition	Calculated transitions		Measured peaks
		Wave length (nm)	Oscillator strength	
Didemnimide A	$\pi \rightarrow \pi^*$	464	0.3805	431
	$\pi \rightarrow \pi^*$	324	0.1053	332
	$\pi \rightarrow \pi^*$	265	0.1279	275
	$\pi \rightarrow \pi^*$	258	0.1995	–
	$\pi \rightarrow \pi^*$	232	0.5629	217
Didemnimide D	$\pi \rightarrow \pi^*$	449	0.3840	419
	$\pi \rightarrow \pi^*$	325	0.1165	334
	$\pi \rightarrow \pi^*$	270	0.1697	298
	$\pi \rightarrow \pi^*$	257	0.2193	288
	$\pi \rightarrow \pi^*$	237	0.1639	–
	$\pi \rightarrow \pi^*$	236	0.1906	–
	$\pi \rightarrow \pi^*$	229	0.6709	222
Didemnimide E	$\pi \rightarrow \pi^*$	394	0.4460	355
	$\pi \rightarrow \pi^*$	296	0.2043	295
	$\pi \rightarrow \pi^*$	255	0.2422	283
	$\pi \rightarrow \pi^*$	227	0.3690	–
	$\pi \rightarrow \pi^*$	218	0.4037	214
	$n_\pi \rightarrow \pi^*$	213	0.2022	–
	$\pi \rightarrow \pi^*$	208	0.3417	–
Isogranulatimide	$\pi \rightarrow \pi^*$	473	0.1602	466
	$\pi \rightarrow \pi^*$	383	0.1411	337
	$\pi \rightarrow \pi^*$	267	0.5913	304
	$\pi \rightarrow \pi^*$	256	0.2084	280
	$\pi \rightarrow \pi^*$	252	0.3856	–
	$\pi \rightarrow \sigma^*$	234	0.1044	–
	$\pi \rightarrow \sigma^*$, π^{*a}	233	0.6031	226
Granulatimide	$\pi \rightarrow \pi^*$	377	0.0100	385
	$\pi \rightarrow \pi^*$	312	0.1105	–
	$\pi \rightarrow \pi^*$	297	0.4524	301
	$\pi \rightarrow \pi^*$	274	0.6723	277
	$\pi \rightarrow \pi^*$	254	0.4800	–
	$\pi \rightarrow \pi^*$	218	0.3847	–
	$\pi \rightarrow \pi^*$	213	0.5571	204

[a] Some mixing of quasi-σ and quasi-π may appear for the non-planar molecule.

checkpoint inhibitors. The largest dipole moment (6.3 debye) is found for granulatimide, while the most stable conformation adopted by the compound didemnimide A reduces the dipole moment to 2.4 debye.

4.2. Electronic spectra

The $\Delta\epsilon$ values are almost constant for all compounds. Therefore, the wavelength of the first electronic transition should be in the same spectral region for all compounds. Indeed, CI calculations indicated that all alkaloids show a first absorption between 377 and 473 nm. The nature of the transitions and oscillator strength values can be seen in Table 2. The last theoretical transition shown occurs at 213 nm for the compound granulatimide. With exception of the transition at 213 nm for the compound didemnimide E which has an $n_\pi \rightarrow \pi^*$ nature, all the other transitions observed for the various compounds

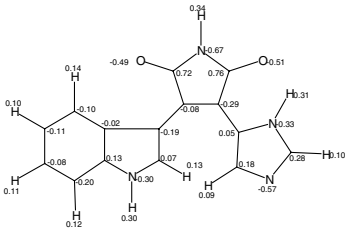

Didemnimide A

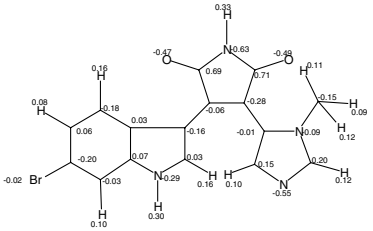

Didemnimide D

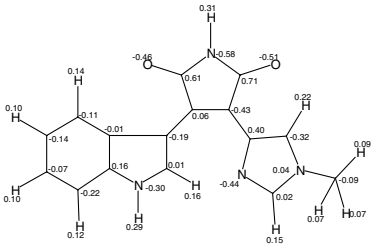

Didemnimide E

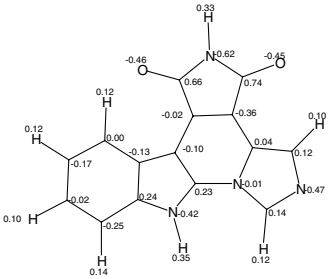

Isogranulatimide

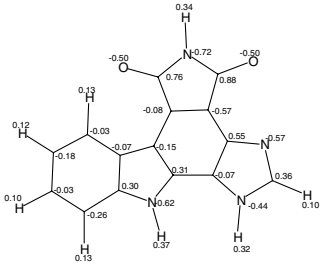

Granulatimide

Fig. 2. Atomic charges for the five compounds analyzed.

present a $\pi \rightarrow \pi^*$ character, and the first lowest transition for all them is HOMO → LUMO. The second transition for didemnimide A, didemnimide D, and isogranulatimide is HOMO → LUMO + 1. The compounds didemnimide E and granulatimide have the second lowest transition HOMO − 1 → LUMO + 1.

The calculated transitions (Table 2) showed a good agreement with the experimental values of electronic absorption for compounds (1)–(5). With the exception of didemnimide E, which shows the first experimental transition at λ_{max} 355 nm, the other alkaloids present the first transition in the range of 377 and 473 nm: isogranulatimide (λ_{max} 466 nm), granulatimide (λ_{max} 385 nm), didemnimide A (λ_{max} 431 nm) and didemnimide D (λ_{max} 419 nm). Two or three other transitions occur in the range between 280 and 340 nm: isogranulatimide (λ_{max} 280, 304, and 337 nm), granulatimide (λ_{max} 301 and 277 nm), didemnimide A (λ_{max} 332 and 275 nm), didemnimide D (λ_{max} 288, 298, and 334 nm), didemnimide E (λ_{max} 283 and 295 nm). Finally, the last transition for each

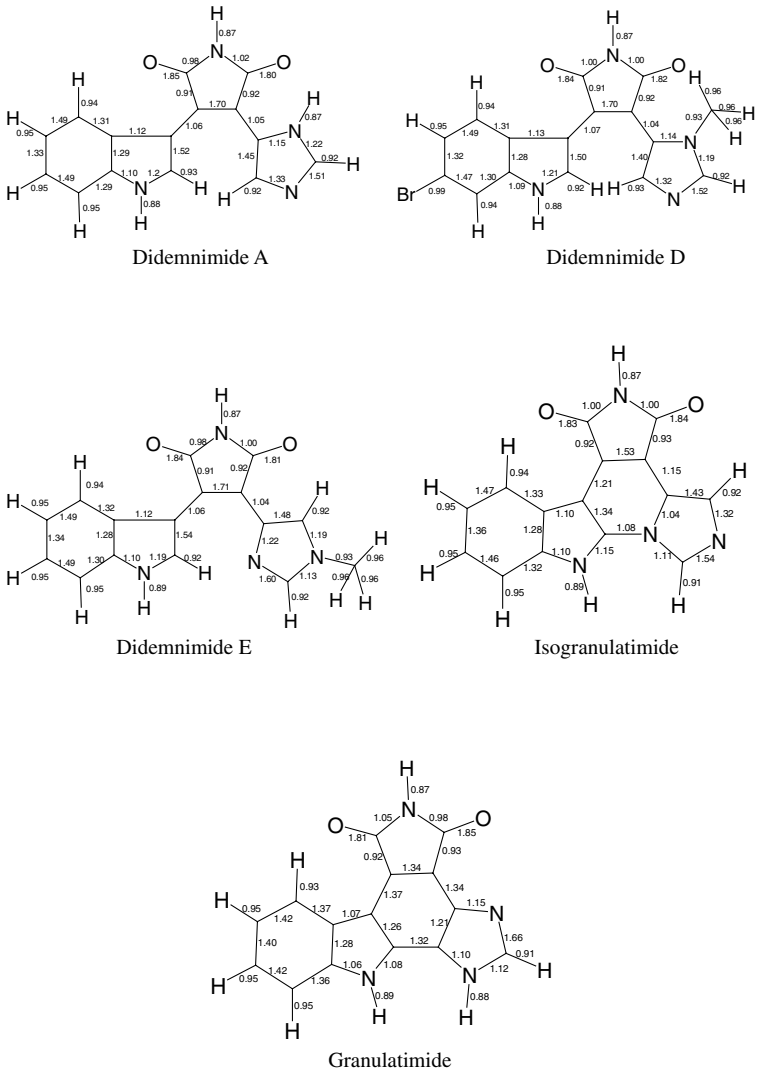

Fig. 3. Bond orders for the *D. granulatum* alkaloids.

molecule occurs below 225 nm: isogranulatimide (λ_{max} 207 and 226 nm), granulatimide (λ_{max} 204 nm), didemnimide A (λ_{max} 217 nm), didemnimide D (λ_{max} 222 nm) and didemnimide E (λ_{max} 214 nm).

4.3. Population analysis

The charge densities derived from the electrostatic potential with the routine AM1 are shown in Fig. 2. The oxygen atom appears as highly polarized for all compounds. The oxygen charges vary from −0.46 to −0.51. The oxygen bonded to C_{11} displays more negative charge values than the oxygen bonded to C_9. The exception is granulatimide, which presents the same partial charges on the two oxygen atoms.

The hydrogen atoms bonded to both N_1 and N_{10} atoms for all compounds show a high positive charge (Fig. 2). The hydrogen bonded to the N_1 nitrogen has a larger positive value in compounds granulatimide and isogralunatimide. The enhancement of the acidity of both N–H hydrogens is clearly due to the aromatic

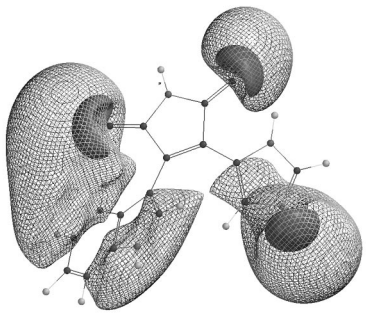

Didemnimide A

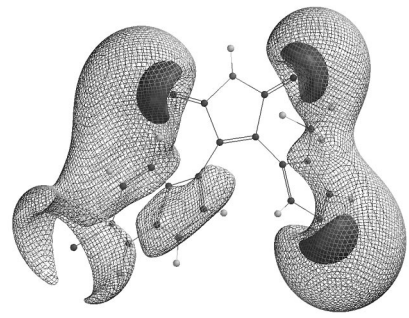

Didemnimide D

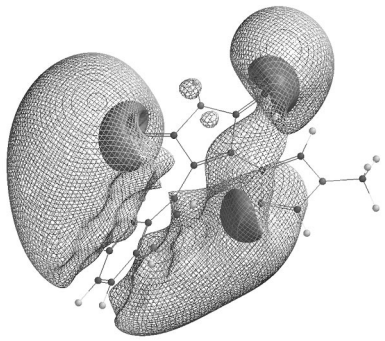

Didemnimide E

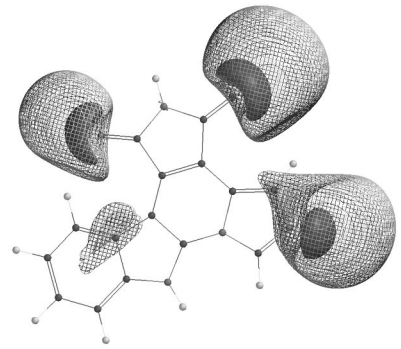

Isogranulatimide

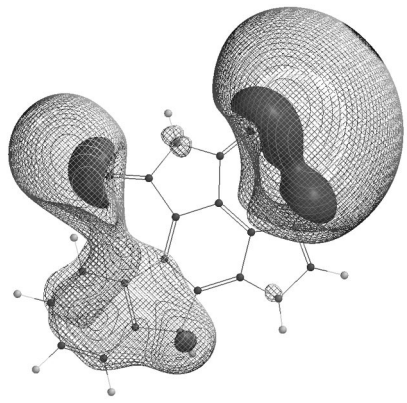

Granulatimide

Fig. 4. Three-dimensional isoenergy contours of MEP for the five compounds. Mesh and solid contours have −10 and −50 kcal/mol electrostatic interaction energy, respectively.

character of the pentacyclic system, which stabilizes the deportonation via charge delocalization. Therefore, the biological activity displayed by isogranulatimide (1) and granulatimide (2) (Fig. 1) may be a consequence of their planarity and their acidic character, factors that may be crucial in binding with the receptor responsible for the inhibition of the G2 cell cycle checkpoint. When the N_{15} and N_{17} nitrogen atoms are bonded to a methyl group, or bonded to another carbon atom, their charges are nearly zero. However, when N_{15} and/or N_{17} are bonded to hydrogen atoms, or participating in the resonance electron delocalization of the imidazole ring, their charges are very negative. The bromine charge for the compound didemnimide D is nearly zero.

Fig. 3 shows the bond order values for all compounds. Both carbonyl groups of all alkaloids have almost a formal double bond character. The pyrrole moiety of indole, as well as the imidazole ring, exhibit bond orders from single to aromatic characters. The presence of the methyl group does not modify markedly the bond orders of the imidazole ring in didemnimide D and didemnimide E when compared with didemnimide A.

4.4. Heat of formation

The AM1 heat of formation of isogranulatimide is 22.1 kcal/mol higher than for granulatimide, and the other compounds have heat of formation values ranging between those. These results suggest that the structure of the granulatimide compound is thermodynamically more stable than the structure of isogranulatimide. However, all compounds have a positive heat of formation. This indicates a certain instability character for all of them.

4.5. The molecular electrostatic potential and biological activity

The three-dimensional MEP maps of the five compounds superimposed onto total electron density show that the lowest electrostatic potential can be found in the proximity of the oxygen atoms of the maleimide ring and nitrogen atoms of the imidazole ring. It is worth to mention that only one of the nitrogen atoms of the imidazole ring presents a very low electrostatic potential. On the other hand, the center with the most positive potential lies near the N_1 and N_{10} nitrogen atoms, except for granulatimide that has negative potential at the N_1 atom. Both isogranulatimide and granulatimide have the most positive value onto the edge hydrogen bonded to the N_1 nitrogen atom. Granulatimide has the most negative charge on the N_1 nitrogen. The plane of the indole ring remains with a negative electrostatic potential for all molecules, whereas the plane of the maleimide ring remains with a positive potential.

However, on examination of the three-dimensional MEP maps beyond the edge of the van der Waals surface (Fig. 4) to account for long-range interactions, two characteristic features are observed. First of all, the planar conformation for the cell cycle checkpoint inhibitors granulatimide and isogranulatimide shows a very large negative potential region extending laterally from the two sides of the active molecules and a positive potential in the central part. In addition, the electrostatic potential is symmetric with respect to the plane of the molecules. Secondly, the didemnimide alkaloids, with no activity as cell cycle checkpoint inhibitors, have a large negative potential in the central part, which is absent for the active molecules. Furthermore, the negative potential of didemnimides does not present any symmetry plane in the inactive molecules.

The large lateral negative potential on the two sides of the active molecules may be regarded as a nucleophilic suction-pump [21], acting as a possible magnet toward the electrophilic part of a receptor. This potential is probably the first portion of the molecule that is recognized by a receptor. This electrostatic interaction may be considered as the driving force toward the formation of a non-covalent Michaelis type of complex with the receptor. Furthermore, the lateral negative potential on the two sides of the active molecules and the positive potential in their central part account for the high polarity of both isogranulatimide and granulatimide: both compounds are completely insoluble in solvents such as acetone, methylene chloride, chloroform or isopropanol, sparingly soluble in methanol or water, but are soluble in ethanol, dimethylsulfoxide and dimethylformamide. On the other hand, the inactive molecules (didemnimides) have a more pronounced lipophilic character than the active molecules (both isogranulatimide and granulatimide), probably due to the large hydrophobic (negative potential) or high-electron density [22] over their overall structure. These results also agree

with the log *P* calculation made with SPARTAN with the Dixon routine (Table 1).

5. Conclusions

Semiempirical AM1 calculations for isogranulatimide (1), granulatimide (2), didemnimide A (3), didemnimide D (4) and didemnimide E (5) (Fig. 1) have been performed. All the frontier molecular orbitals and deeper orbitals are of π symmetry and scattered in several sites over the rings. The LUMO orbitals are mainly localized in the C_2 and C_8 carbon atoms. Considering all five *D. granulatum* alkaloids studied herein, both the HOMO and LUMO energies are in the range of 0.6–0.8 eV.

The electronic charges derived from the electrostatic potential and bond indexes for all compounds have been calculated as well. The hydrogen atoms bonded to the N_1 nitrogen atom have a higher value of electronic charge in the biologically active compounds than for inactive compounds.

Investigation of the electronic features of *D. granulatum* alkaloids isogranulatimide (1), granulatimide (2) and didemnimides A (3), D (4), and E (5) (Fig. 1), aiming to understand the key structural characteristics responsible for the activity as G2 cell cycle checkpoint inhibitors, resulted in the following profile: the molecular planarity creates a broad electrostatic potential on the two sides of the active molecules isogranulatimide and granulatimide, with a plane of symmetry and a positive potential in their central core. The positive potential resulting from a low electron density in the central core of both isogranulatimide and granulatimide increases their hydrophilicity, while the negative potential on their sides creates two lypophilic sites. The inactive didemnimides A, D, and E are more lypophilic than the active molecules, due to the high-electron density in the central regions that enhance their hydrophobicity. Therefore, we conclude that the steric factors control electronic features that should be directly related to biological activity.

The electronic spectra for the various compounds were also calculated and measured.

Acknowledgements

The authors are gratefully indebted to Professor Raymond J. Andersen (Department of Chemistry, University of British Columbia, Vancouver, BC, Canada) for providing a sample of synthetic granulatimide. R.G.S.B. thanks Fundação de Amparo à Pesquisa do Estado de São Paulo (FAPESP) for a visiting professor fellowship at the University of British Columbia (97/06799-6). Financial support by FAPESP grants 96/04316-5, 98/09060-4 and the American Society of Pharmacognosy Research Starter Grant (1998) to R.G.S.B. is acknowledged. J.H.H.L.O. thanks CNPq for a MSc Scholarship. A.J.C. and M.T. also thank CNPq and FINEP (Brazilian agencies) for financial support.

References

[1] C.M. Ireland, D.M. Roll, T.F. Molinski, T.C. McKee, T.M. Zabriskie, J.C. Swersey, in: D.G. Fautin (Ed.), Biomedical Importance of Marine Organisms, California Academy of Sciences, San Francisco, 1988, pp. 41–57.
[2] B.S. Davidson, Chem. Rev. 93 (1993) 1771–1791.
[3] T.F. Molinski, Chem. Rev. 93 (1993) 1825–1838.
[4] C.M. Ireland, B.R. Copp, M.P. Foster, L.A. McDonald, D.C. Radisky, J.C. Swersey, in: D.H. Attaway, O.R. Zaborsky (Eds.), Marine Biotechnology, vol. I, Plenum, New York, 1993, pp. 1–43.
[5] D.J. Watters, A.L. van den Brenk, Toxicon 31 (1993) 1349–1372.
[6] G.R. Dietzmann, in: J.P. Devlin (Ed.), High Throughput Screening, Marcel Dekker, New York, 1997 (p. 99).
[7] R.G.S. Berlinck, R. Britton, E. Piers, L. Lim, M. Roberge, R.M. Rocha, R.J. Andersen, J. Org. Chem. 63 (1998) 9850–9856.
[8] M. Roberge, R.G.S. Berlinck, L. Xu, H. Anderson, L.Y. Lim, D. Curman, C.M. Stringer, S.H. Friend, P. Davies, I. Vincent, S.J. Haggarty, M.T. Kelly, R. Britton, E. Piers, R.J. Andersen, Cancer Res. 58 (1998) 5701–5706.
[9] H.C. Vervoort, S.E. Richard-Gross, W. Fenical, A.Y. Lee, J. Clardy, J. Org. Chem. 62 (1997) 1486–1490.
[10] SPARTAN 5.0, Wavefunction, Inc., Irvine, CA, 1997.
[11] M. Clark, R.D. Cramer III, N.V. Opdensch, J. Comput. Chem. 10 (1989) 982.
[12] M.J.S. Dewar, E.G. Zoebisch, E.F. Healy, J.J.P. Stewart, J. Am. Chem. Soc. 107 (1985) 1285.
[13] AMPAC 5.0, Semichem, Inc., 1994.
[14] D.E. Williams, J. Yan, Adv. Atomic Mol. Phys. 23 (1998) 87.
[15] L.E. Chirlian, M.M. Francl, J. Comput. Chem. 8 (1987) 894.
[16] F. Momany, J. Phys. Chem. 82 (1978) 592.

[17] S.R. Cox, D.E. Williams, J. Comput. Chem. 2 (1981) 304.
[18] M.L. Connolly, J. Appl. Crystallogr. 16 (1983) 548.
[19] U.C. Singh, P.A. Kollman, J. Comput. Chem. 5 (1984) 129.
[20] D.E. Williams, J. Comput. Chem. 15 (1994) 719.
[21] J. Lamottebrasseur, G. Dive, Dehareng, J.M. Ghuysen, J. Theoret. Biol. 145 (1990) 183.
[22] Y.S. Lee, R. Pearlstein, P.F. Kador, J. Med. Chem. 37 (1994) 787.